Medicinal Chemistry Research
https://doi.org/10.1007/s00044-018-2198-5

MEDICINAL CHEMISTRY RESEARCH

ORIGINAL RESEARCH

# Design, synthesis, and biological evaluation of Cyclobentinib (CB1107) as a potential anti-CML agent

Zijun Zhou[1] · Yang Wang[1] · Jun Li[1] · Baichun Hu[2] · Xiaolin Lin[1] · Ye Chen[1] · Rui Wang[1] · Ju Liu[1] · Hongsheng Liu[1]

Received: 13 March 2018 / Accepted: 25 May 2018


## Abstract

Cyclobentinib was designed and synthesized as a novel anti-CML agent, its in vitro activity against K562 cells was evaluated by MTT assay. CB1107 showed remarkable cytotoxicity against K562 cell line with an $IC_{50}$ of 0.037 ± 0.028 μmol/L, and thus it was 17-fold more potent than the reference drug Imatinib. Inducing cell apoptosis and affecting cell cycling of this compound in K562 cells were estimated by using flow cytometry and Acridine Orange/Ethidium Bromide (AO/EB) staining. The results showed that CB1107 was capable of arresting cell cycle at G0/G1 phase as well as inducing cell apoptosis significantly. Molecular mechanism of CB1107 was detected by the protein expression of Bcr-$Abl^{P210}$ using western blotting analysis. Downregulation of expression of Bcr-$Abl^{P210}$ was obviously revealed in the treatment of this tetralin amide compound. Of note, the results of these investigations suggested that CB1107 is more potent than the reference drug Imatinib against K562 cells. Additionally, in vivo results indicated that CB1107 significantly decreased tumor growth in K562 tumor-bearing Non-obese Diabetic/Severe Combined Immunodeficiency (NOD/SCID) mice. Histopathological investigation revealed that CB1107 without notable toxicity in a given dose range. These findings collectively demonstrate CB1107 is a promising candidate as a novel anti-CML agent.

**Keywords** CML · Bcr-Abl · Cyclobentinib (CB1107) · K562 · Biological activity

## Introduction

Chronic myelogenous leukemia (CML) was well known to be associated with a characteristic chromosomal translocation called the Philadelphia chromosome (Druker 2008; Strick et al. 2006). This translocation causes the expression of constitutively activated break-point cluster region-Abelson (Bcr-Abl) tyrosine kinase, and this deregulated tyrosine kinase control the cell cycle, speeding up cell division as well as inhibit apoptosis reduced by many intracellular signaling pathways (e.g., SRC pathway, Ras/Raf pathway, MAPK pathway, JAK/STAT signaling pathway, and PI3K pathway) (Park et al. 2012; Hasford et al. 2003; Gesbert and Griffin 2000; Fruman et al. 1998; Campbell et al. 1998; McCubrey et al. 2007; Downward 2003).

Imatinib mesylate as the first ATP-site targeting agent, specifically inhibit the activity of the Bcr-Abl tyrosine kinase, which have led to dramatically improved long-term survival rates of patients with CML(Hasselbalch et al. 2003; Bennasroune et al. 2004). Imatinib mesylate is the first-line treatment for chronic myeloid leukemia (Jabbour 2016), but a proportion of patients develops resistance to imatinib or cannot tolerate its side effects. (Deangelo and Attar 2010; Yamada et al. 2011; Scheinfeld 2006). Update, a large effort is ongoing to develop more secondary and tertiary Bcr-Abl tyrosine kinase inhibitors (Giles et al. 2013; Tauchi and Ohyashiki 2006), such as Nilotinib (Kantarjian et al. 2007), Dasatinib (Quintas-Cardama et al. 2007) and Ponatinib (Shamroe and Comeau 2013) (Fig. 1), that were approved by FDA, are able to overcome such point mutantions within the Bcr-Abl catalytic domain. Although these new generation inhibitors applied in patients with mutation, their strong side effects make the patient's life hardly extended,

**Electronic supplementary material** The online version of this article (https://doi.org/10.1007/s00044-018-2198-5) contains supplementary material, which is available to authorized users.

✉ Ye Chen
sy-chenye@163.com

[1] School of Pharmacy, Liaoning University, Liaoning 110036 Shenyang, China

[2] Key Laboratory of Structure-Based Drug Design & Discovery of Ministry of Education, School of Pharmaceutical Engineering, Shenyang Pharmaceutical University, 110016 Shenyang, China

Published online: 15 June 2018

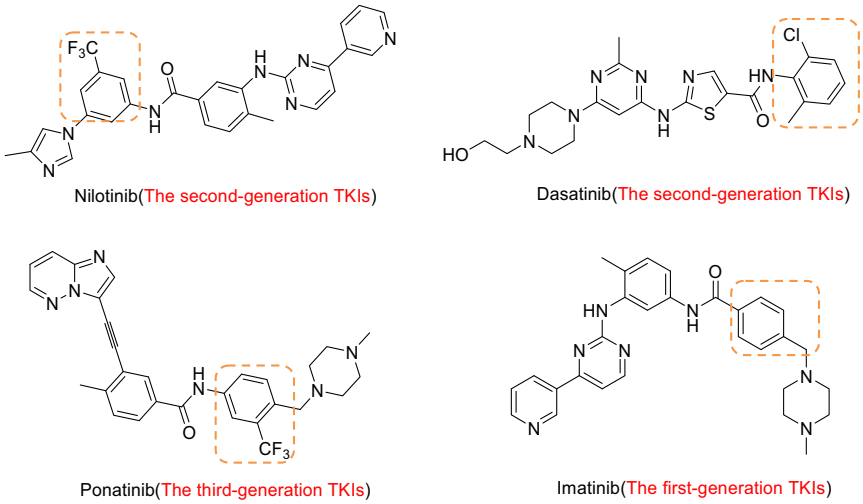


**Fig. 1** Chemical structures of FDA-approved Bcr-Abl inhibitors (orange-dashed frame indicate the group of drugs, which is able to enter the hydrophobic region of ATP-binding site)

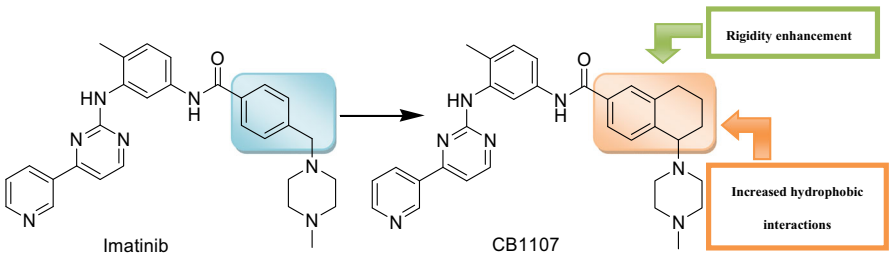


**Fig. 2** The design of target compound from Imatinib

inducing other Bcr-Abl kinase domain mutations as well (Lau and Seiter 2014; Douxfils et al. 2016; Soverini et al. 2009; Haguet et al. 2017; Modugno 2014; FDA Drug Safety Commol/Lunication. U.S. Food and Drug Administration 2013).

As shown in Fig. 1, secondary and tertiary Bcr-Abl tyrosine kinase inhibitors were added a new group in benzamide-core of Imatinib, such as trifluoromethyl, which allows this part to be better into the hydrophobic region of the binding site (Stierand and Rarey 2010). Thus, it is desirable to obtain a more active agent by replacing the benzamide-core with a tetrahydronaphthalene-core (Fig. 2). A molecular docking study of this compound was performed against the c-Abl kinase domain (PDB ID: 3K5V) with the comparision of the reference structure (Imatinib) by using *X*-score (Fig. 3). The scores of the compound was −12.51 and the reference drug Imatinib was −11.33. This results indicated that CB1107 binding to the c-Abl kinase domain active site was more tighter than Imatinib. Moreover, the docking results analysis showed that CB1107 had strong affinity to the ATP-site by forming hydrogen bond with five important amino acid residues (MET337, THR334, ASP400, GLU305, and MET309, the former four amino acid were the shared amino acid with Imatinib). Besides, the structural optimization leads to the increased hydrophobic interactions between tetrahydronaphthalene part and the hydrophobic region of ATP-site (VAL398, LEU317, LEU373, and HIS380), which account for increased affinity in kinase domain active site. In addition, this cyclization modification induced rigidity enhancement of target compound, which stabilize the active conformation of the compound. As shown in this docking results, the structural modification enhances the affinity of the small molecule compound to the target. Therefore, we synthesized and evaluated the anti-CML activity of this tetrahydronaphthalene amide-type compound.

## Experimental

### Chemistry part

All reagents and solvents used were purchased from commol/Lercial suppliers and were used without further purification. Spectral data were recorded as follows: Perkin Elmer (FT-IR); Agilent 1100 liquid Chromatograph-Electron Spray Ionization-High Resolution Mass Spectrometer (LC-ESI-HRMS); Bruker AVANCE 600 ($^{1}$H Nuclear Magnetic Resonance (NMR), $^{13}$C NMR). The synthetic route for the preparation of CB1107 is illustrated in Scheme 1. The structure of target compound was characterized by IR, $^{1}$H NMR, $^{13}$C NMR, LC-ESI-HRMS.

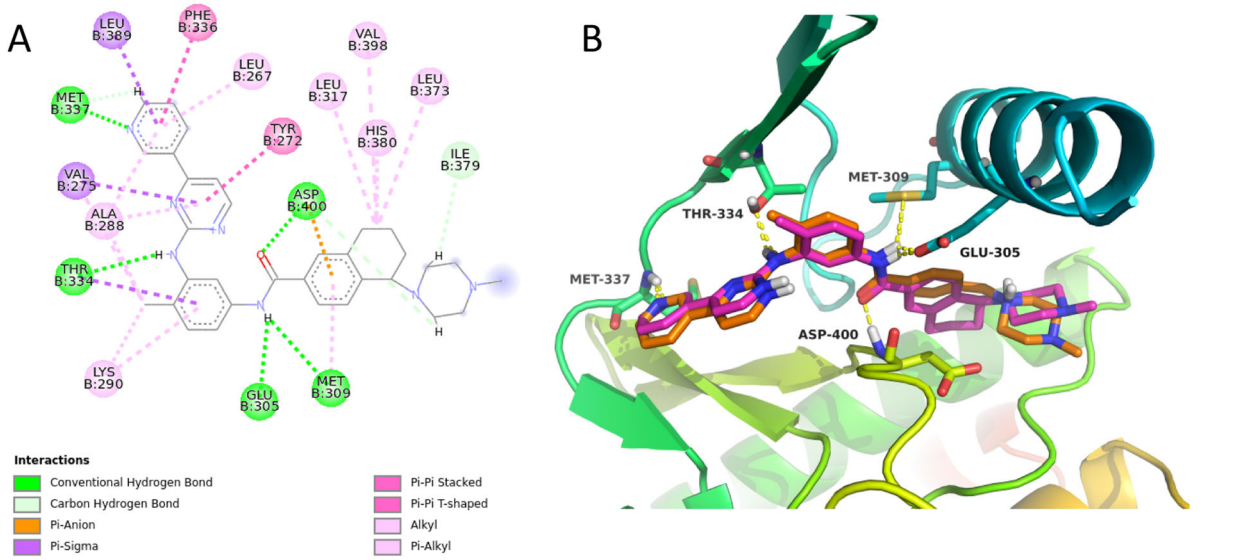


**Fig. 3** **a** Schematic diagram of interactions of CB1107 to c-Abl kinase domain site. **b** PyMOL cartoon representation of docking result for CB1107 (pink) in c-Abl ATP-binding site. Imatinib (orange) is used as reference molecule. For the sake of clarity, only polar hydrons are displayed; and only the amino acids that generate H-bonds are shown as lines

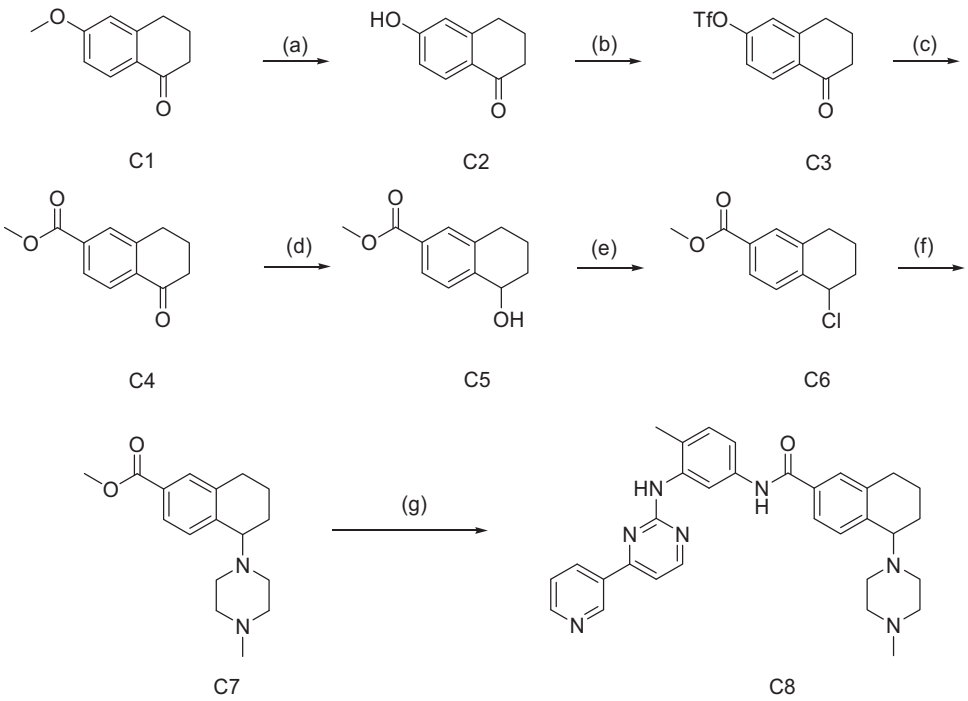


**Scheme 1** Synthetic route for CB1107. Reagents and conditions: (**a**) 48% HBr, 100 °C, 24 h; (**b**) trifluoromethanesulfonic anhydride, triethylamine, $CH_2Cl_2$; (**c**) palladium acetate, 1,3-bis(diphenylphosphino) propane, CO, DMF, 65 °C, 22 h; (**d**) sodium borohydride, methyl alcohol, rt; (**e**) thionyl chloride, $CH_2Cl_2$, rt; (**f**) DMF, *N*-methyl piperazine, potassium carbonate, 50 °C, 6 h; (**g**) *N*-(5-Amino-2-methylphenyl)-4-(3-pyridyl)-2-pyrimidineamine, trimethylaluminum, 100 °C, 6 h

### Synthesis of 6-hydroxy-3,4-dihydronaphthalen-1 (2H)-one (C2)

The reaction mixture of 6-methoxy-3,4-dihydronaphthalen-1 (2H)-one (17.6 g, 100 mmol/L) and 40% hydrobromic acid aqueous solution (100 mL) was stirred at 100 °C for 24 h and then cooled to room temperature. The reaction solution was added to ice water to stir a large amount of solid to precipitate. The solid was filtered and washed with 5% carbonic acid aqueous solution of sodium hydride, and then washed with deionized water to neutral and dried. The crude product was purified by silica gel column eluting with ethyl acetate: *n*-hexane = 1:5.

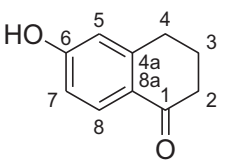

Yield: 13.9 g (86.0%).$^1$H NMR (600 MHz, DMSO-$d_6$) $\delta$ 10.29 (s, 1H, OH-6), 7.74 (d, $J = 8.6$ Hz, 1H, H-8), 6.71 (dd, $J = 8.6$, 2.4 Hz, 1H, H-7), 6.65 (d, $J = 2.4$ Hz, 1H, H-5), 2.83 (t, $J = 6.0$ Hz, 2H, H-4), 2.49–2.46 (t, 2H, H-2), 2.09–1.87 (m, 2H, H-3); $^{13}$C NMR (151 MHz, DMSO-$d_6$) $\delta$ 196.20(C-1), 162.37(C-6), 147.56(C-4a), 129.37(C-8), 124.95(C-8a), 114.64(C-7), 114.57(C-5), 38.76(C-2), 29.59 (C-4), 23.36(C-3).

### Synthesis of 5-oxo-5,6,7,8-tetrahydronaphthalen-2-yl trifluoromethanesulfonate (C3)

A solution of 6-hydroxy-1-naphtholone (8.1 g, 50 mmol/L) was dissolved in dichloromethane (50 mL), and then 20 mL dichloromethane solution of $Tf_2O$ (14.1 g) was slowly dropwised into the mixture, followed by 20 mL dichloromethane containing tris ethylamine (5.05 g) was dropwised. The reaction mixture was allowed to stand at room temperature for 2 h. Next, the reaction solution was washed two times with dilute $NaHCO_3$ solution and two times with brine. The organic phase was dried over anhydrous sodium sulfate, filtered, and concentrated.

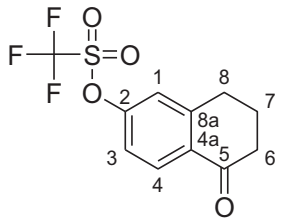


Yield: 13.97 g (95.2%).$^1$H NMR (600 MHz, $CDCl_3$) $\delta$ 8.13 (d, $J = 8.5$ Hz, 1H, H-4), 7.20 (m, 2H, H-1, 3), 3.02 (t, $J = 6.1$ Hz, 2H, H-8), 2.69 (t, $J = 12.7$, 2H, H-6), 2.19 (dt, $J = 12.7$, 6.1 Hz, 2H, H-7); $^{13}$C NMR (151 MHz, $CDCl_3$) $\delta$ 196.30(C-5), 152.25(C-2), 147.03(C-8a), 132.29(C-4), 129.93(C-4a), 121.27($CF_3$), 119.63(C-1), 119.58(C-3), 38.68(C-6), 29.64(C-8), 22.82(C-7).

### Synthesis of methyl 5-oxo-5,6,7,8-tetrahydronaphthalene-2-carboxylate (C4)

5-oxo-5,6,7,8-tetrahydronaphthalen-2-yl trifluoromethanesulfonate (11.8 g, 40 mmol/L) was dissolved in methanol (50 mL) and then DMF (5 mL), DIEA (*N*,*N*-diisopropylethylamine) (5 mL), palladium acetate (4 g), and Dppp [1,3-bis(diphenylphosphine)propane] (4 g) were added. After the reaction system was sealed and vacuumed, the reaction was carried out under carbon monoxide atmosphere at a temperature of 65 °C for 22 h. The reaction solution was filtered through celite and the filtrate was concentrated, followed by dissolving it in 200 mL ethyl acetate and washed three times with brine. The organic phase was dried and filtered. The filtrate was concentrated under reduced pressure and separated by column chromatography to obtain product C4.

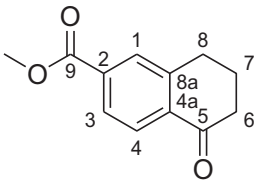


Yield: 5.3 g (65.0%).$^1$H NMR (600 MHz, $CDCl_3$) $\delta$ 8.08 (d, $J = 8.0$ Hz, 1H, H-4), 7.94 (m, 2H, H-1, 3), 3.94 (s, 3H, $OCH_3$), 3.03 (t, $J = 6.1$ Hz, 2H, H-8), 2.70 (t, $J = 6.0$ Hz, 2H, H-6), 2.20–2.15 (m, $J = 6.1$, 6.0 Hz, 2H, H-7); $^{13}$C NMR (151 MHz, $CDCl_3$) $\delta$ 197.71(C-5), 166.31(C-9), 144.25(C-8a), 135.45(C-4a), 133.86(C-2), 130.12(C-1), 127.35(C-4), 127.23(C-3), 52.37($OCH_3$), 39.06(C-6), 29.52 (C-8), 22.97(C-7).

### Synthesis of methyl 5-hydroxy-5,6,7,8-tetrahydronaphthalene-2-carboxylate (C5)

Methyl 5-oxo-5,6,7,8-tetrahydronaphthalene-2-carboxylate (4.08 g, 20 mmol/L) was dissolved in methanol (50 mL), and then $NaBH_4$ (0.76 g, 20 mmol/L) was slowly added in it. The reaction mixture was stirred at room temperature for 3 h. The reaction solution was concentrated under reduced pressure, followed by dissolving it in 50 mL ethyl acetate and washed two times with brine. The organic phase was dried and filtered. The filtrate was concentrated under reduced pressure to obtain product C5.

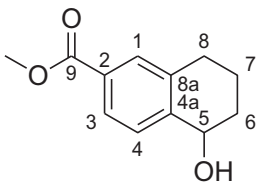


Yield: 4.1 g (99.5%).$^1$H NMR (600 MHz, $CDCl_3$) $\delta$ 7.84 (d, $J = 8.1$ Hz, 1H, H-4), 7.78 (s, 1H, H-1), 7.52 (d, $J = 8.1$ Hz, 1H, H-3), 4.79 (t, $J = 5.4$ Hz, 1H, H-5), 3.90 (s, 3H, $OCH_3$), 2.81 (m, 2H, H-8), 2.05–1.95 (m, 2H, H-6), 1.92–1.77 (m, 2H, H-7); $^{13}$C NMR (151 MHz, $CDCl_3$) $\delta$ 167.02(C-9), 143.74(C-4a), 137.14(C-8a), 130.18(C-1), 128.99(C-4), 128.37(C-2), 127.05(C-3), 67.97(C-5), 51.99 ($OCH_3$), 32.10(C-6), 29.04(C-8), 18.86(C-7).

### Synthesis of methyl 5-chloro-5,6,7,8-tetrahydronaphthalene-2-carboxylate (C6)

Methyl 5-hydroxy-5,6,7,8-tetrahydronaphthalene-2-carboxylate (3.09 g, 15 mmol/L) was dissolved in dichloromethane (20 mL), and then 10 mL dichloromethane solution of $SOCl_2$ (7.08 g, 60 mmol/L) was slowly dropwised into the

mixture at 0–5 °C. The reaction mixture was allowed to stand at room temperature for 6 h. The reaction solution was concentrated under reduced pressure, followed by dissolving it in 50 mL ethyl acetate and washed two times with brine. The organic phase was dried and filtered. The filtrate was concentrated under reduced pressure to obtain product C6. Yield: 3.18 g (94.5%). C6 was used directly in the next step.

### Synthesis of methyl 5-(4-methylpiperazin-1-yl)-5,6,7,8-tetrahydronaphthalene-2-carboxylate (C7)

Methyl 5-chloro-5,6,7,8-tetrahydronaphthalene-2-carboxylate (2.41 g, 10 mmol/L) was dissolved in DMF (20 mL), $K_2CO_3$ (2.78 g, 20 mmol/L), and *N*-methylpiperazine (2 g, 20 mmol/L) were added as well. After 5 h at 50 °C, 80 mL ethyl acetate was added to the reaction solution and adjusted to neutralization by using dilute aqueous hydrochloric acid, the organic phase was washed with brine, dried, and filtered, and the organic solvent taken off. The product was obtained by the separation of silica gel column chromatography (methanol: dichloromethane = 30:1).

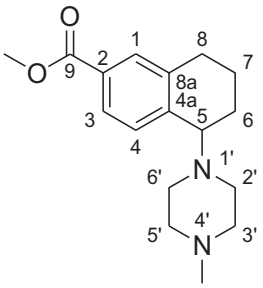


Yield: 2.12 g (73.9%).$^1$H NMR (600 MHz, $CDCl_3$) $\delta$ 7.79 (d, $J = 8.2$ Hz, 1H, H-4), 7.77 (d, $J = 8.2$ Hz, 1H, H-3), 7.74 (s, 1H, H-1), 3.89 (s, 3H, $OCH_3$), 3.83 (t, $J = 8.9$ Hz, 1H, H-5), 2.78 (dt, $J = 8.9$, 8.0 Hz, 2H, H-8), 2.52 (d, $J = 37.9$ Hz, 8H, H-2′,3′,5′,6′), 2.32 (s, 3H, CH3), 2.00 (m, $J = 10.1$, 8.0 Hz, 2H, H-7), 1.69 (t, $J = 10.1$ Hz, 2H, H-7); $^{13}$C NMR (151 MHz, $CDCl_3$) $\delta$ 21.027(C-7), 21.597(C-6), 29.497(C-8), 45.967(CH3), 51.858($OCH_3$), 55.641(C-2′,C-6′), 62.721(C-3′,C-5′), 126.585(C-3), 127.935(C-2), 128.005(C-4), 130.032 (C-1), 138.400(C-8a), 143.638(C-4a), 167.247(C-9).

### Synthesis of *N*-(4-methyl-3-(4-(pyridin-3-yl)pyrimidin-2-ylaminp)phenyl)-5-(4-methylpiperazin-1-yl)-5,6,7,8-terahydronaphthalene-2-carboxamide (C8)

Methyl 5-(4-methylpiperazin-1-yl)-5,6,7,8-tetrahydronaphthalene-2-carboxylate (2.88 g, 10 mmol/L) and *N*-(5-amino-2-methylphenyl)-4-(3-pyridyl)-2-pyrimidineamine (3.32 g, 12 mmol/L) was suspended in 30 mL toluene and 5 mL toluene solution of 2.0 mol/L trimethylaluminum was added and reacted at 100 °C for 6 h. After the solution was cooled, 50 mL potassium tartrate aqueous solution was added with stirring. The solution was extracted three times with ethyl acetate (100, 100, 50 mL). The extracts were combined and washed with $NaHCO_3$ solution (100 mL) and brine (100, 100, 50 mL), dried, and filtered, and the filtrate was concentrated under reduced pressure and separated by silica gel column chromatography.

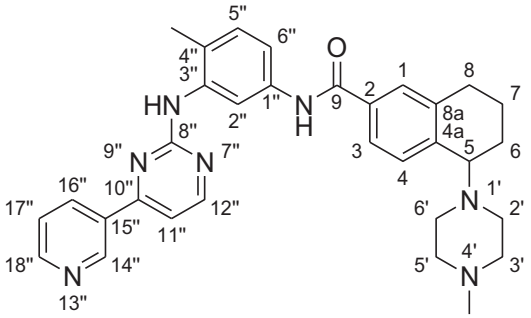


Yield: 2.32 g (43.5%). Purity: 99.86%; $^1$H NMR (600 MHz, $CDCl_3$) $\delta$ 9.23 (d, $J = 1.8$ Hz, 1H, –CONH–), 8.54 (s, 1H, H-14″), 8.45 (m, 2H, H-11″, 16″), 8.16 (s, 1H, H-2″), 7.76 (d, $J = 7.8$ Hz, 1H, H-18″), 7.64 (d, $J = 8.8$ Hz, 1H, H-12″), 7.58 (s, 1H, H-1), 7.40 (dd, $J = 7.8$ Hz, 4.8 Hz, 1H, H-17″), 7.32 (dd, $J = 7.8$ Hz, 1.8 Hz, 1H, H-6″), 7.18 (d, $J = 7.8$ Hz, 1H, H-5″), 7.13 (m, 2H, H-3,4), 3.83 (m, 1H, H-5), 3.00–2.41 (m, 10 H, H-2′,3′,5′,6′,8), 2.36 (s, 3H, $CH_3$-4″), 2.32 (s, 3H, $CH_3$-N), 1.98 (m, 2H, H-6), 1.67 (m, 2H, H-7), $^{13}$C NMR (151 MHz, $CDCl_3$) $\delta$ 17.607(Ar-$CH_3$), 21.091(C-7), 21.612(C-6), 29.653(C-8), 55.668(C-2′,6′,5), 62.632(C-3,5′), 108.302(C-2″,11″), 112.919(C-6″), 115.124 (C-17″), 123.666(C-4″), 123.982(C-3), 124.029(C-1), 127.518(C-4,5″), 128.444(C-2), 130.719(C-15″), 132.631(C-16″), 132.959(C-1″), 134.870(C-8a), 136.585(C-4a), 137.714(C-3″), 138.901(C-18″), 148.448(C-14″), 151.430(C-12″), 158.973(C-10″), 160.520(C-9), 165.547(C-8″); Infrared Radiation (IR) (KBr, $cm^{-1}$): 3417, 2930, 2797, 1648, 1581, 1528, 1450, 1319, 1285, 1193, 1135, 1009; HRMS (ESI) *m/z* (%): 534.2977 $[M + H]^+$, 556.2798 $[M + Na]^+$.

## Biological part

### Cell culture

K562 cells (provided by Shanghai Institution for Biological Sciences) were grown in RPMI-1640 supplemented with 10% fetal bovine serum, 100 U/mL penicillin, and 100 mg/mL streptomycin. The cultures were maintained at 37 °C in a humidified atmosphere with 5% $CO_2$. Cells in the exponential growth phase were used for all the experiments.

### MTT viability assay

MTT viability assay was performed to examine the toxicity of compounds on K562 cells. K562 cells were seeded in 96-

well plate at a density of about $1 \times 10^5$ cells per well. In order to enhance the solubility in aqueous solution, CB1107 was prepared in the form of mesylate salt. After culture for 24 h, K562 cells were exposed to escalating concentrations (range from 50 μmol/L to $5 \times 10^{-6}$ μmol/L) of CB1107 and the reference drug Imatinib. After 48 h incubation at 37 °C in a humidified atmosphere with 5% $CO_2$, 20 μL MTT solution (5 mg/mL, pH = 7.4, PBS was the solvent) was added to each well and incubated for another 4 h. A centrifugal treatment with 96-well plate, the culture medium was then removed. The plate was added with 150 μL DMSO per well, shaken for 10 min for crystal dissolution. The optical density (OD) of each well was measured using a microtiter plate reader at a wave length of 490 nm. Cellular proliferation inhibition rate was calculated as follows: inhibition rate (%) = [1-$OD_{490}$ (treated)/$OD_{490}$(control)] × 100%.

### Cell-cycle analysis by flow cytometry

Cell cycling was measured by propidium iodide (PI) staining. K562 cells were seeded in six-well plate at a density of about $1 \times 10^6$ cells per well. After culture for 24 h, the cells were treated with CB1107 and Imatinib. After 48 h incubation at 37 °C in a humidified atmosphere with 5% $CO_2$, control cells and treated cells were collected, washed with PBS, and fixed with 70% ethanol overnight on ice. Then, the ethanol-suspended cells were centrifuged, washed with PBS, and stained with PI for 30 min at room temperature, followed by measuring of cell fluorescence.

### Apoptosis analysis by flow cytometry

Apoptosis was measured by flow cytometry using annexin V/PI double staining. K562 cells were seeded in six-well plate at a density of about $1 \times 10^6$ cells per well. After culture for 24 h, the cells were treated with CB1107 and Imatinib. Cells were cultured in the presence of indicated concentrations of drugs for 48 h, collected and washed, and then resuspended in 100 μL 1× binding buffer incubated in the mixture of 5 μL annexin V-FTIC and 5 μL PI for 10 min at room temperature in dark place. The cells were resuspended in 400 μL 1× binding buffer just before flow cytometric analysis.

### AO/EB staining

AO/EB staining were performed to observe the morphologic changes in the treatment of CB1107 and Imatinib by fluorescene microscopy. K562 cells were added to a final concentration of $1 \times 10^6$/mL in a 24-well plate, and the plate was incubated for 24 h. Cells were treated with CB1107 and Imatinib. After being cultured for 48 h, cells were collected, washed with PBS that stored at 4 °C, and then dual fluorescent staining solution (1 μL) containing 100 μg/mL AO and 100 μg/mL EB was added to each suspension for 10 min, and then covered with a coverslip. The morphology of apoptotic cells was examined using fluorescent microscope.

### Western blotting analysis

The treated cells were collected, washed with PBS which stored at 4 °C and RIPA buffer (20 mmol/L Tris/HCl (pH 7.5), 150 mmol/L NaCl, 1 mmol/L sodium EDTA, 1 mmol/L EGTA, 1% Triton, 2.5 mmol/L sodium pyrophosphate, 1 mmol/L 2-glycerophosphate, 1 mmol/L sodium orthovanadate, 1 μg/mL leupeptin, and 1 mmol/L PMSF) was used to lyse the cells on ice for 1 h. The cell lysates were then centrifuged at 12,000 r.p.m. for 10 min at 4 °C. The cleared supernatants were collected and protein concentrations were quantified by a BCA (bicinchoninic acid) assay. Different amounts of the reference protein were fractionated by SDS-PAGE (6% gradient gels) and then transferred on to a PVDF membrane by wet electroblotting. The membrane was blocked with 20% BSA for 2 h and incubated with the primary antibody (Bcr-Abl rabbit poly-antibody) and the secondary horseradish-peroxidase conjugated antibody. Finally, bound antibody was detected with an Electrochemiluminescence (ECL) detection system.

### In vivo evaluation of CB1107 in the treatment of K562 human chronic myelogenous leukemia xenografts in (NOD/SCID) mice

NOD/SCID mice with body weight ranging from 18 to 22 g were provided by Beijing HFK Bioscience Co., Ltd. Animals were allowed free access to tap water and food in the form of a standard pellet diet. Each mouse was inoculated subcutaneously at the right flank with K562 tumor cells ($1 \times 10^7$) in 200 μL of PBS/Matrigel (1:1) for tumor development. The treatment of CB1107 were started at day 7 after tumor inoculation when the tumor size reached ~260 $mm^3$. Each group consisted of 10 mice. CB1107 was dissolved in 0.9% NaCl and administered via oral gavage at dosages of 80 and 40 mg/kg, twice daily, for 21 days, in comparison with the treatment of Imatinib at 100 mg/kg. The major endpoint was to see if the tumor growth can be delayed or mice can be cured. Tumor size was measured twice weekly in two dimensions using a caliper, and the volume was expressed in $mm^3$ using the formula: $V = 0.5a \times b^2$, where $a$ and $b$ are the long and short diameters of the tumor, respectively. The tumor size was then used for calculations of both $T$–$C$ and $T/C$ values. $T$–$C$ was calculated with $T$ as the median time (in days) required for the treatment group tumors to reach a predetermined size (e.g.,

1000 $mm^3$), and *C* as the median time (in days) for the control group tumors to reach the same size. The *T*/*C* value (in percent) was an indication of antitumor effectiveness; *T* and *C* were the mean volume of the treated and control groups, respectively, on a given day. Additionally, pathological section was made, and the pathological change was observed by a light microscope.

### Statistical analysis

The collected data are presented as means ± SD from at least three sets of measurements. The assumptions underlying the analysis of variance were met and the statistical difference between the control and treated groups was evaluated by using IBM SPSS Statistics 20. $p < 0.05$ and below was considered to be statistically significant.

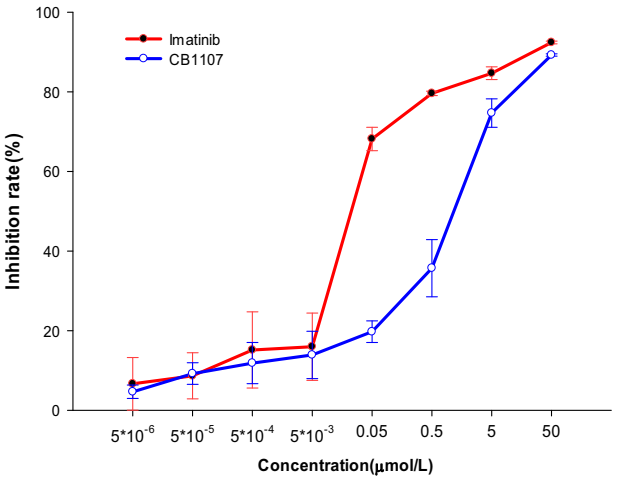


**Fig. 4** Inhibitory effects of CB1107 in comparison to the reference drug Imatinib on K562 cells

## Results and discussion

### Chemistry

As shown in Scheme 1, 6-methoxy-3,4-dihydronaphthalen-1 (2H)-one (**C1**), which as a starting material, was hydroxylated to give 6-hydroxy-3,4-dihydronaphthalen-1 (2H)-one (**C2**). Next, 6-hydroxy was protected by trifluoromethanesulfonic acid, and then it was esterified to obtain methyl 5-oxo-5,6,7,8-tetrahydronaphthalene-2-carboxylate (**C4**), followed by 5-carbonyl reduction reaction. The intermediate (**C5**) was catalyzed by $SOCl_2$ to generate **C6**. Methyl 5-(4-methylpiperazin-1-yl)-5,6,7,8-tetrahydronaphthalene-2-carboxylate (**C7**) was formed by a nucleophilic substitution of *N*-methylpiperazine and **C6**. The desired tetrahydronaphthalene amide-type **C8** (CB1107) was resulted in the reaction of methyl 5-(4-methylpiperazin-1-yl)-5,6,7,8-tetrahydronaphthalene-2-carboxylate (**C7**) and *N*-(5-Amino-2-methylphenyl)-4-(3-pyridyl)-2-pyrimidineamine that were catalyzed by toluene solution of trimethylaluminum.

### Biological evaluation

In the present work, the inhibitory effect of CB1107 on the proliferation of K562 leukemia cancer cells in vitro was evaluated by MTT assay. The results showed that CB1107 significantly inhibited the growth of K562 cells in a dose-dependent manner (Fig. 4). The $IC_{50}$ value of CB1107 was 0.037 ± 0.028 μmol/L. Descriptive data were expressed as mean ± standard deviation and the $IC_{50}$ value of drugs were carried out using IBM SPSS statistics 19.

In order to shed some light on the mechanism responsible for the antiproliferative properties, investigations were carried out. As we all know, there is a fundamental link between regulation of the cell cycle and cancer, because of the over-expressed products of tumor suppressor genes that are critically involved in cell-cycle regulation, that control the passage of cells from G1 to S phase. Therefore, we further investigated cell-cycle progression in treated K562 cells. After exposing K562 cells to three concentrations (10, 1, and 0.1 μmol/L) of drugs for 48 h, cell-cycle analysis was conducted by using flow cytometry with PI staining, followed by measuring of cell fluorescence. As seen in Fig. 5, cell-cycle progression were markedly arrested in the G0/G1 phase with a concomitant dose-dependent decrease in the populations of S- and G2/M-phase cells.

The induction of apoptosis in human leukemia K562 cells after exposition to CB1107 and Imatinib was investigated using flow cytometry after staining with annexin V/Fluorescein Isothiocyanate (FITC) and PI. The treated cells were stressed with drugs for 48 h, remarkable apoptosis was observed in K562 cells compared with control, as seen in Fig. 6. Apoptosis-inducing effects of CB1107 were more potent than the reference drug. In addition, AO/EB staining were performed to observe the morphologic changes of apoptosis by fluorescene microscopy after the cells were treatment with drugs for 48 h. All cells can be permeated by AO and the nuclei appear green. EB is only taken up by cells when cytoplasmic membrane integrity is lost, and the nucleus can be stained in red. As shown in Fig. 7, almost all cell nucleus of untreated control group were stained in green; most cells in the treatment of three different concentrations of CB1107 displayed cell volume becomes larger, bright green nucleus with condensed chromatin (at early phases of apoptosis), or condensed orange chromatin (at last phases of apoptosis) accompanied by the appearance of apoptotic bodies in green, and cells in the treatment of 10 and 1 μmol/L of Imatinib showed the same morphology. However, K562 cells in the treatment of 0.1 μmol/L of

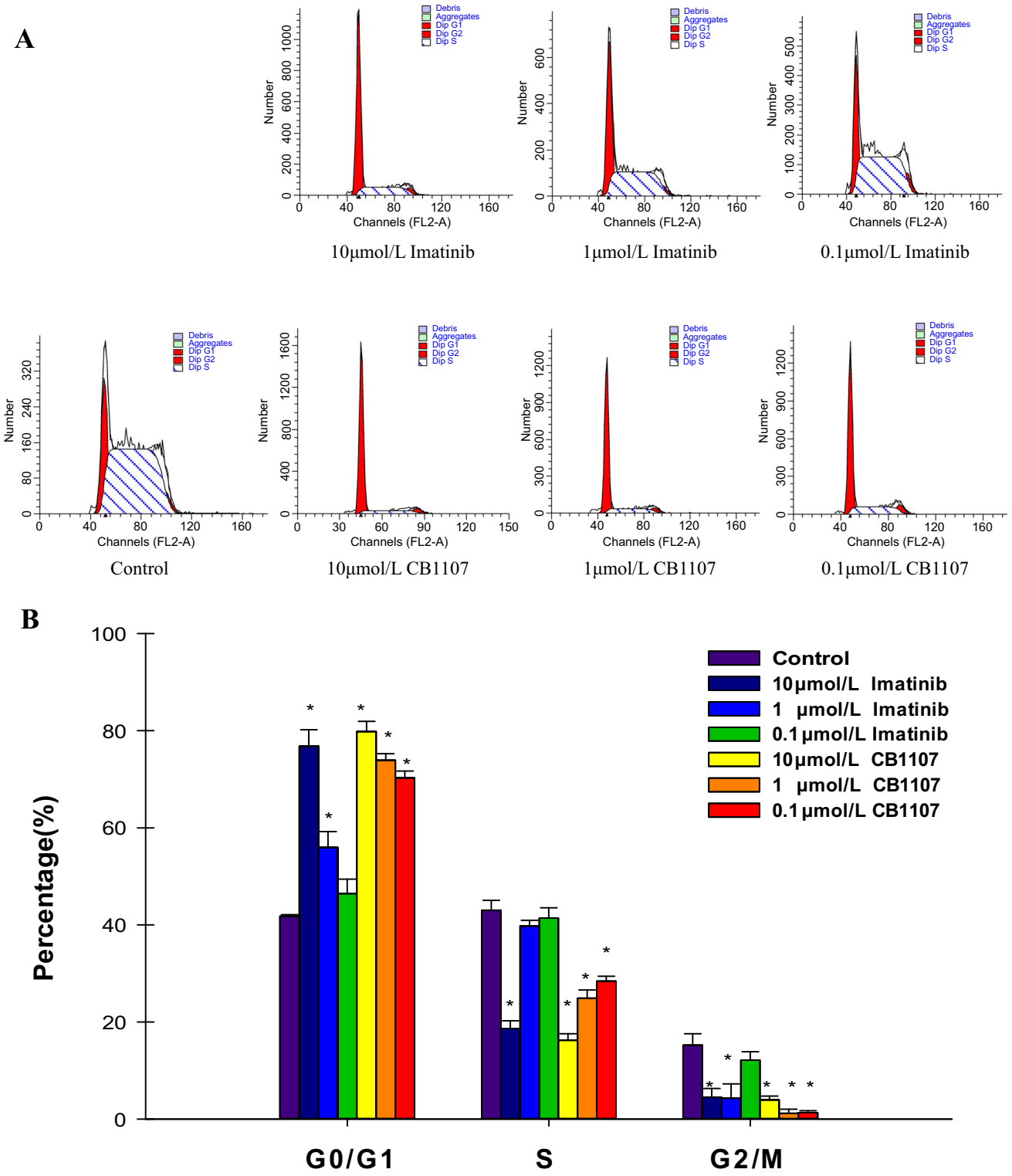


**Fig. 5** Effects of CB1107 and Imatinib on the K562 cells cycle. Cells were treated with CB1107 and Imatinib (10, 1, and 0.1 μmol/L) for 48 h. **a** Effects of CB1107 and Imatinib on the cell-cycle distribution of K562 cells. **b** Quantitative analysis of cell-cycle phase. (*) indicate significant difference ($p < 0.05$); analysis of variance (ANOVA) followed by Dunnett's test compared with control group

Imatinib only had less bright green or orange nucleus with condensed chromatin, and a small part of cells were accompanied by the appearance of apoptotic bodies. These morphological observation results were comformed with that detected using flow cytometry. Briefly, the results demonstrated that CB1107 could prevent the proliferation

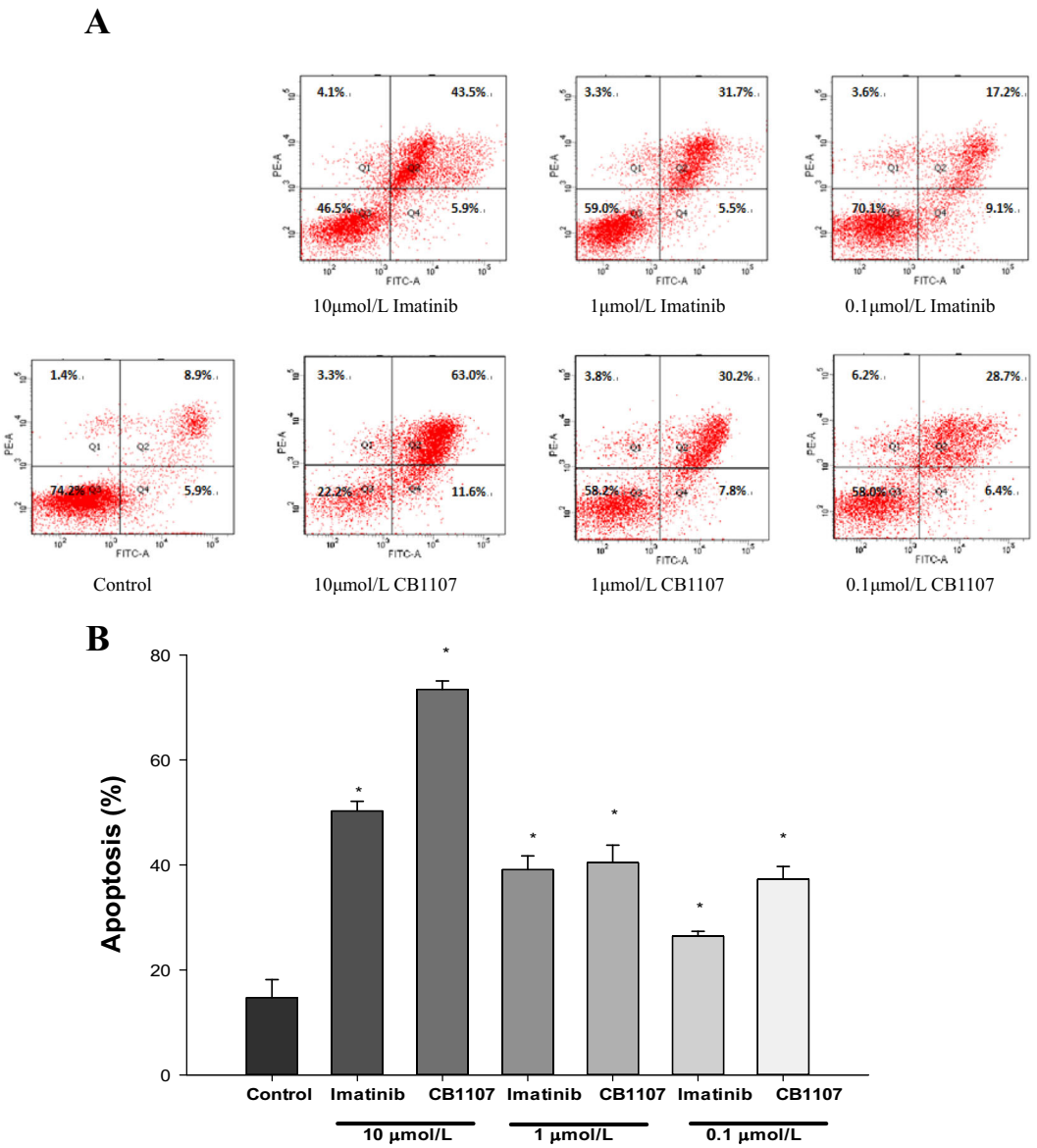


**Fig. 6** Effects of CB1107 and Imatinib on the K562 cells. The K562 cells were treated with CB1107 and Imatinib (10, 1, and 0.1 μmol/L) for 48 h. **a** Apoptosis was determined by annexin V-FITC/PI staining by flow cytometry. **b** Quantitative analysis of apoptotic cells. (*) indicate significant difference ($p < 0.05$); analysis of variance (ANOVA) followed by Dunnett's test compared with control group

of cancer cells by arresting the cell cycle and induce G0/G1 arrest accompanied by apoptosis in K562 cells.

Bcr-Abl protein is an attractive target for CML therapies, it was the target protein of our drug design of CB1107 as well. Therefore, we investigated its expression in the human CML cell line K562 cells, which were treated with CB1107, and Imatinib was used as a reference compound. The results showed that downregulation of expression of Bcr-Abl$^{P210}$ was obviously revealed in the treatment of CB1107 and its effect was stronger than the reference drug, Imatinib (Fig. 8).

According to our in vitro data, CB1107 showed significant inhibitory activity, effective apoptosis induction, and cell-cycle arrest in K562 cells, as well as significant changes in expression of Bcr-Abl protein. Therefore, we further investigated the effect of CB1107 in vivo as a single agent in the treatment of K562 human CML xenografts in NOD/SCID mice. Animals were treated by CB1107 at 80 and 40 mg/kg, with the reference drug Imatinib at 100 mg/kg, for 21 days during the experiment period based on the body weight change. Antitumor activity of CB1107 in the treatment of K562 human leukemia xenografts was shown in Table 1. The results of tumor sizes in different groups at different time points after tumor inoculation are shown in the Fig. 9a. The mean tumor size of the vehicle treated control mice reached 1346 mm$^3$ at day 20 after tumor

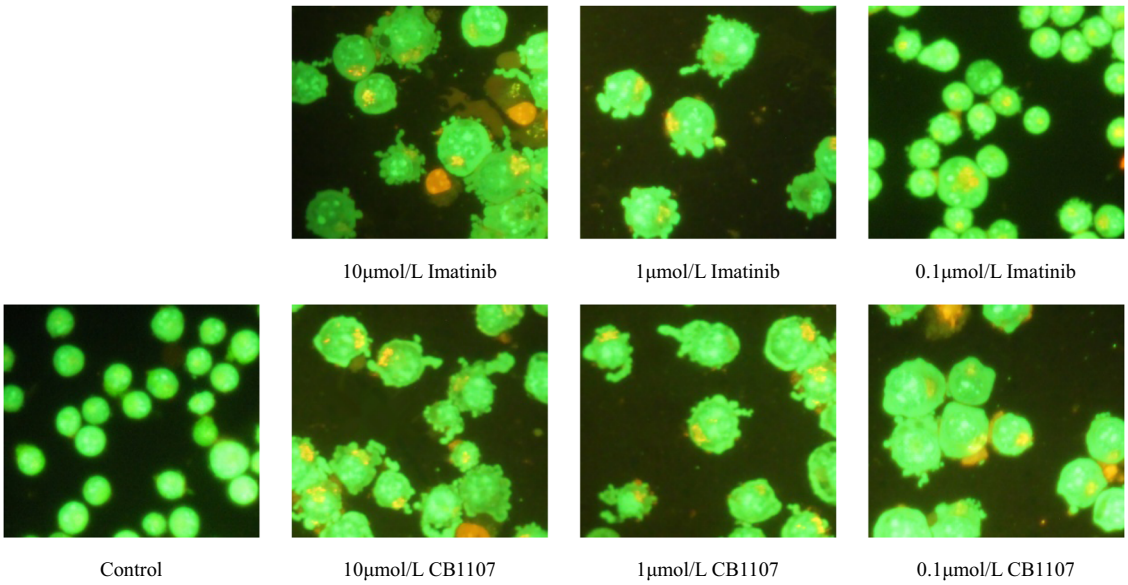


**Fig. 7** The AO/EB staining of CB1107 and Imatinib in K562 cells. Magnification ×400

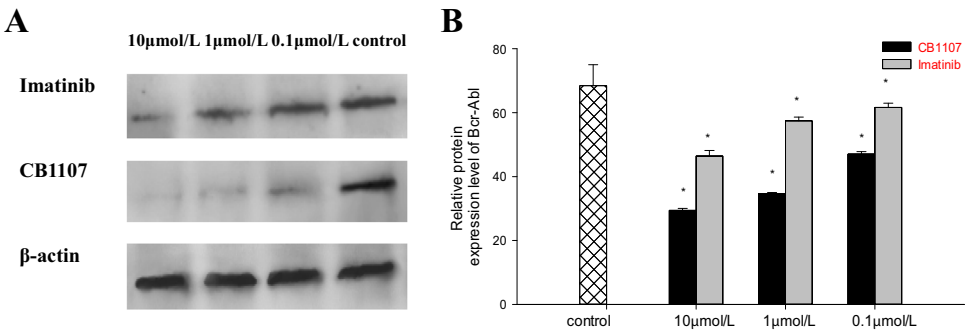


**Fig. 8** **(a)** Effects of Imatinib and CB1107 on the expression levels of Bcr-Abl protein by western blotting in K562 cells for 48 h. **(b)** Relative quantity expression profile of Bcr-Abl protein. (*) indicate significant difference ($p < 0.05$); analysis of variance (ANOVA) followed by Dunnett's test compared with control group

**Table 1** Antitumor activity of CB1107 in the treatment of K562 human leukemia xenografts

| Treatment | Tumor size ($mm^3$) At day 20 | *T/C* (%) | *T–C* (days) At 1000 $mm^3$ | *p* value |
|---|---|---|---|---|
| PBS | 1346 ± 313 | — | — | — |
| CB1107 (80 mg/kg) | 0 | 0 | >3 | 0.002 |
| CB1107 (40 mg/kg) | 0 | 0 | >3 | 0.001 |

inoculation. Treatment with the test article CB1107 at dose levels of 80 and 40 mg/kg (adjusted to the body weight changes of animals), twice daily, produced a significant antitumor activity, their mean tumor sizes were 46 $mm^3$ at the same time (*T/C* value = 3.41%; $p = 0.002$) with the tumor growth delays of more than 3 days at tumor size of 1000 $mm^3$ compared with the vehicle group 1. The animals in CB1107 treated group had a remarkable body weight loss (>20%) after treatments (Fig. 9b) and two mice died of compound toxicity. In summary, CB1107 as a single agent produced a significant antitumor activity against the K562 human CML xenografts model in this study. However, two mice died during the treatment suggesting that CB1107 had clear toxicity at the applied dose in this study. Histopathological investigation was carried out after the animals were treated with CB1107 at specified doses for 21 days (Fig. 9c). From the histological section, hydropic degeneration in the hepatic tissue and pus focal sectretion in the lung were found in treated group. Other organs including heart, spleen, and kidney showed no sign of pathological changes compared to the corresponding organs from the animals in the control group. The animals in the convalescence group were killed after 30-day recovery period without drug treatment. The pathological differences of lung disappeared after the recovery period, and there was no pathological changes from these animals that could be detected by either naked eyes or histological dissection.

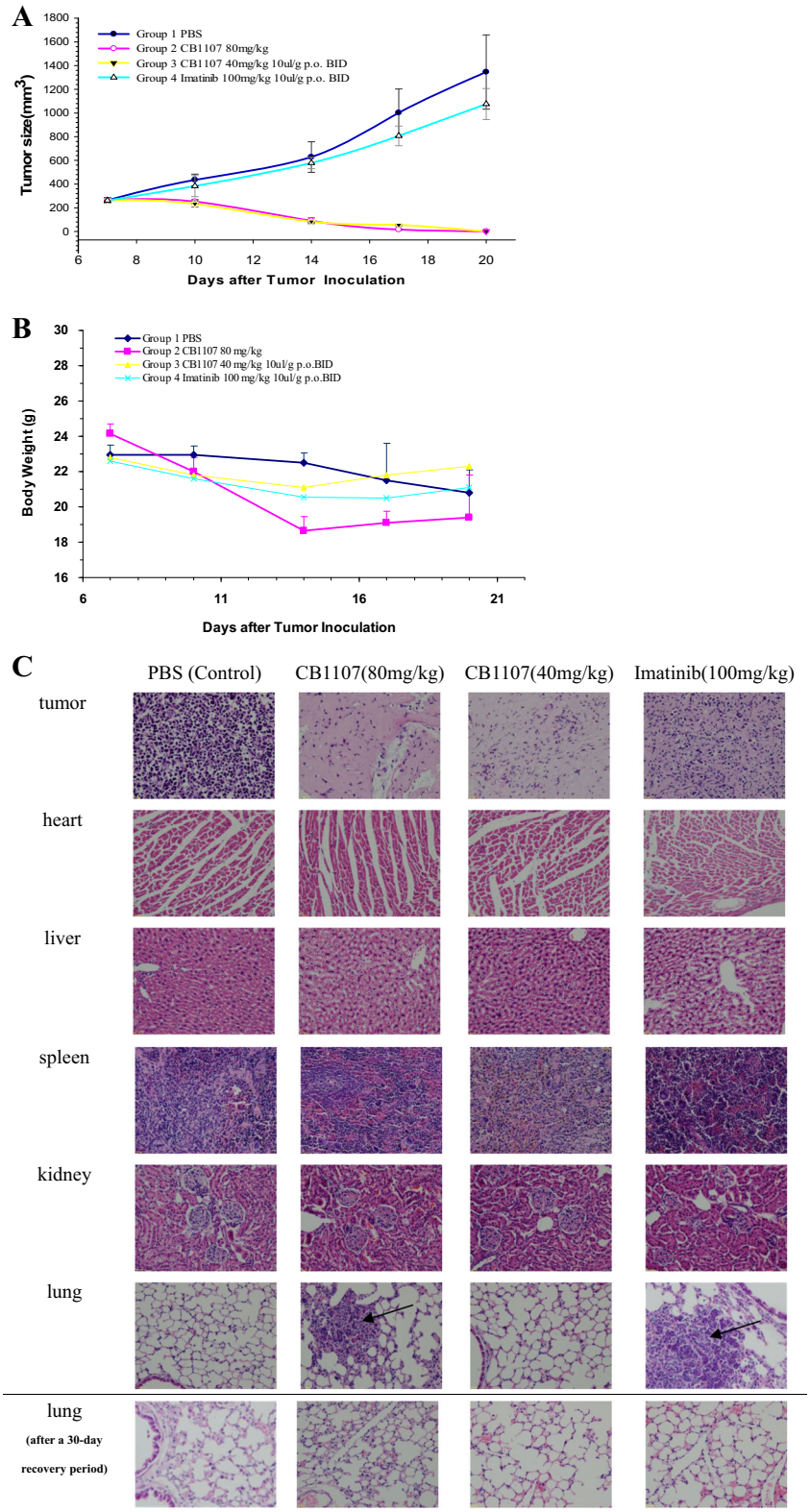


**Fig. 9** **(a)** Tumor sizes of K562 xenograft tumor model in the treatment of CB1107. **(b)** The body weight changes of K562 tumor-bearing animals caused by CB1107 treatment. **(c)** The pathology sections of tumor and organs in the control group and treatment groups

## Conclusion

In this present study, Cyclobentinib (CB1107) were designed, synthesized, and tested for its anticancer activity. It exhibited significant antiproliferative activity against K562 cells (human CML cell line) with an $IC_{50}$ of 0.037 ± 0.028 μmol/L. The results of flow cytometric assays showed that most K562 cells were blocked to progress through S-

phase and arrested at G0/G1 phase with the treatment of CB1107. Inducing cell apoptosis of this compound in K562 cells were estimated by using flow cytometry and AO/EB staining. These results revealed that the percentage of apoptotic K562 cells was increased after CB1107 treatment for 48 h. Briefly, CB1107 has great pro-apoptotic potential. This is an important finding because apoptosis is one of the most important pathways used in targeting the discovery of new anticancer drug. Western blot analysis showed that the expression level of Bcr-Abl protein was markedly decreased. Of note, the results of these investigations suggested that CB1107 is more potent and effective than the reference drug Imatinib. In addition, further investigations to confirm anti-CML efficacy in vivo was performed in the model of K562 tumor-bearing NOD/SCID mice. The results indicated that CB1107 had significant antitumor activity and its inhibitory effect was more potent than Imatinib. Histopathological investigation showed that CB1107 and Imatinib-treated group all have some pathological changes in lung tissue. But these changes were disappeared after the recovery period, other organs displayed no pathological changes as well. In summary, pharmacodynamics study result in vivo suggested that CB1107 without notable toxicity in a given dose range.

These findings collectively demonstrate that CB1107 is a promising candidate as a novel anti-CML for further clinical development.

**Acknowledgements** This work was supported by the Department of Science and Technology of Shenyang Government (F16-182-9-00) and Innovation Team Project from the Education Department of Liaoning province (no.: LT2015011).

## Compliance with ethical standards

**Conflict of interest** The authors declare that they have no conflict of interest.

## References

Bennasroune A, Gardin A, Aunis D, Crémel G, Hubert P (2004) Tyrosine kinase receptors as attractive targets of cancer therapy. Crit Rev Oncol Hematol 50:23–38

Campbell SL, Khosravi-Far R, Rossman KL, Clark GJ, Der CJ (1998) Increasing complexity of Ras signaling. Oncogene 17:1395–1413

Deangelo DJ, Attar EC (2010) Use of dasatinib and nilotinib in imatinib-resistant chronic myeloid leukemia: translating preclinical findings to clinical practice. Leuk Lymphoma 51:363–375

Douxfils J, Haguet H, Mullier F, Chatelain C, Graux C, Dogné JM (2016) Association between BCR-ABL tyrosine kinase inhibitors for chronic myeloid leukemia and cardiovascular events, major molecular response, and overall survival: a systematic review and meta-analysis. JAMA Oncol 22:625-632

Downward J (2003) Targeting RAS signalling pathways in cancer therapy. Nat Rev Cancer 3:11–22

Druker BJ (2008) Translation of the Philadelphia chromosome into therapy for CML. Blood 112:4808–4817

FDA Drug Safety Commol/Lunication. U.S. Food and Drug Administration (2013) "FDA asks manufacturer of the leukemia drug Iclusig (ponatinib) to suspend marketing and sales". https://www.fda.gov/Drugs/DrugSafety/ucm373040. Accessed October 31 2013

Fruman DA, Meyers RE, Cantley LC (1998) Phophoinositide kinases. Annu Rev Biochem 67:481–507

Gesbert F, Griffin JD (2000) Bcr/Abl activates transcription of the *Bcl-X* gene through STAT5. Blood 96:2269–2276

Giles FJ, le Coutre PD, Pinilla-Ibarz J, Larson RA, Gattermann N, Ottmann OG, Hochhaus A, Radich JP, Saglio G, Hughes TP, Martinelli G, Kim DW, Novick S, Gillis K, Fan X, Cortes J, Baccarani M, Kantarjian HM (2013) Nilotinib in imatinib-resistant or imatinib-intolerant patients with chronic myeloid leukemia in chronic phase: 48-month follow-up results of a phase II study. Leukemia 27:107–112

Haguet H, Douxfils J, Mullier F, Chatelain C, Graux C, Dogné JM (2017) Risk of arterial and venous occlusive events in chronic myeloid leukemia patients treated with new generation BCR-ABL tyrosine kinase inhibitors: a systematic review and meta-analysis. Expert Opin Drug Saf 16:5–12

Hasford J, Pfirrmann M, Hehlmann R, Baccarani M, Guilhot F, Mahon FX, Kluin-Nelemans HC, Ohnishi K, Thaler J, Steegmann JL, for the Collaborative CML Prognostic Factors Project Group (2003) Prognosis and prognostic factors for patients with chronic myeloid leukemia: nontransplant therapy. Semin Hematol 40:4–12

Hasselbalch HC, Bjerrum OW, Jensen BA, Clausen NT, Hansen PB, Birgens H, Therkildsen MH, Ralfkiaer E (2003) Imatinib mesylate in idiopathic and postpolycythemic myelofibrosis. Am J Hematol 74:238–242

Jabbour E (2016) Chronic myeloid leukemia: first-line drug of choice. Am J Hematol 91:59–66

Kantarjian HM, Giles F, Gattermann N, Bhalla K, Alimena G, Palandri F, Ossenkoppele GJ, Nicolini FE, O'Brien SG, Litzow M, Bhatia R, Cervantes F, Haque A, Shou Y, Resta DJ, Weitzman A, Hochhaus A, le Coutre P (2007) Nilotinib (formerly AMN107), a highly selective BCR-ABL tyrosine kinase inhibitor, is effective in patients with Philadelphia chromosome-positive chronic myelogenous leukemia in chronic phase following imatinib resistance and intolerance. Blood 110:3540–3546

Lau A, Seiter K (2014) Second-line therapy for patients with chronic myeloid leukemia resistant to first-line imatinib. Clin Lymphoma Myeloma Leuk 14:186–196

McCubrey JA, Steelman LS, Chappell WH, Abrams SL, Wong EWT, Chang F, Lehmann B, Terrian DM, Milella M, Tafuri A, Stivala F, Libra M, Basecke J, Evangelisti C, Martelli AM, Franklin RA (2007) Roles of the Raf/MEK/ERK pathway in cell growth, malignant transformation and drug resistance. Biochim Biophys Acta 1773:1263–1284

Modugno M (2014) New resistance mechanisms for small molecule kinase inhibitors of Abl kinase. Drug Discov Today Technol 11:5–10

Park H, Hong S, Hong S (2012) Identification of commol/Lon inhibitors of wild-type and T315I mutant of BCR-ABL through the parallel structure-based virtual screening. J Comput Aided Mol Des 26:983–992

Quintas-Cardama A, Kantarjian H, Jones D, Nicaise C, O'Brien S, Giles F, Talpaz M, Cortes J (2007) Dasatinib (BMS-354825) is active in Philadelphia chromosome-positive chronic myelogenous leukemia after imatinib and nilotinib (AMN107) therapy failure. Blood 109:497–499

Scheinfeld N (2006) Imatinib mesylate and dermatology part 2: a review of the cutaneous side effects of imatinib mesylate. J Drugs Dermatol 5:228–231

Shamroe CL, Comeau JM (2013) Ponatinib: a new tyrosine kinase inhibitor for the treatment of chronic myeloid leukemia and Philadelphia chromosome-positive acute lymphoblastic leukemia. Ann Pharmacother 47:1540–1546

Soverini S, Gnani A, Colarossi S, Castagnetti F, Abruzzese E, Paolini S, Merante S, Orlandi E, de Matteis S, Gozzini A, Iacobucci I, Palandri F, Gugliotta G, Papayannidis C, Poerio A, Amabile M, Cilloni D, Rosti G, Baccarani M, Martinelli G (2009) Philadelphia-positive patients who already harbor imatinib-resistant Bcr-Abl kinase domain mutations have a higher likelihood of developing additional mutations associated with resistance to second- or third-line tyrosine kinase inhibitors. Blood 114:2168–2171

Stierand K, Rarey M (2010) Drawing the PDB: protein−ligand complexes in two dimensions. ACS Med Chem Lett 1:540–545

Strick R, Zhang Y, Emmol/Lanuel N, Strissel PL (2006) Commol/Lon chromatin structures at breakpoint cluster regions may lead to chromosomal translocations found in chronic and acute leukemias. Hum Genet 119:479–495

Tauchi T, Ohyashiki K (2006) The second generation of BCR-ABL tyrosine kinase inhibitors. Int J Hematol 83:294–300

Yamada O, Ozaki K, Furukawa T, Machida M, Wang YH, Motoji T, Mitsuishi T, Akiyama M, Yamada H, Kawauchi K, Matsuoka R (2011) Activation of STAT5 confers imatinib resistance on leukemic cells through the transcription of TERT, and MDR1. Cell Signal 23:1119–1127